CrossMark

TRANSITING THE SUN. II. THE IMPACT OF STELLAR ACTIVITY ON Lyα TRANSITS

J. LLAMA[1,2] AND E. L. SHKOLNIK[1,3]
[1] Lowell Observatory, 1400 W Mars Hill Road, Flagstaff, AZ 86001, USA; joe.llama@lowell.edu
[2] SUPA, School of Physics & Astronomy, North Haugh, St Andrews, Fife KY16 9SS, UK
[3] ASU School of Earth and Space Exploration, Tempe, AZ 85287, USA

ABSTRACT

High-energy observations of the Sun provide an opportunity to test the limits of our ability to accurately measure the properties of transiting exoplanets in the presence of stellar activity. Here we insert the transit of a hot Jupiter into continuous disk integrated data of the Sun in Lyα from NASA's *Solar Dynamics Observatory*/EVE instrument to assess the impact of stellar activity on the measured planet-to-star radius ratio ($R_p/R_\star$). In 75% of our simulated light curves, we measure the correct radius ratio; however, incorrect values can be measured if there is significant short-term variability in the light curve. The maximum measured value of $R_p/R_\star$ is 50% larger than the input value, which is much smaller than the large Lyα transit depths that have been reported in the literature, suggesting that for stars with activity levels comparable to the Sun, stellar activity alone cannot account for these deep transits. We ran simulations without a transit and found that stellar activity cannot mimic the Lyα transit of 55 Cancari b, strengthening the conclusion that this planet has a partially transiting exosphere. We were able to compare our simulations to more active stars by artificially increasing the variability in the Solar Lyα light curve. In the higher variability data, the largest value of $R_p/R_\star$ we measured is $<3\times$ the input value, which again is not large enough to reproduce the Lyα transit depth reported for the more active stars HD 189733 and GJ 436, supporting the interpretation that these planets have extended atmospheres and possible cometary tails.

Key words: planets and satellites: atmospheres – stars: activity – starspots

1. INTRODUCTION

Transiting exoplanets provide the opportunity to explore the atmospheric size and composition of planets outside our own Solar system. Observations in the near- and far-ultraviolet (NUV, FUV) are sensitive to the upper atmosphere of the planet where this radiation is absorbed. Lyα ($\lambda_{Ly\alpha} = 121.6$ nm) emission of neutral hydrogen (H I) is the strongest chromospheric emission feature in the stellar FUV spectrum and the dominant source of UV flux for M dwarfs (Ehrenreich et al. 2011).

Indeed, direct observations of active M dwarfs have revealed a high FUV flux (Shkolnik & Barman 2014) and that the total Lyα flux can be up to 75% of the total UV flux (115–310 nm), far greater than the Solar value of 0.04% (France et al. 2013). Originating in the transition region between the chromosphere and corona, Lyα is used as a proxy for determining both the temperature and pressure profiles of the stellar atmosphere; however, observing Lyα emission from stars is challenging since it is entirely absorbed by the Earth's atmosphere and is heavily effected by absorption in the ISM requiring space-based observations of the nearest stars (Linsky 1980).

Since Lyα emission is absorbed in the upper atmospheres of planets it offers one of the most promising opportunities to infer the presence of extended atmospheres of exoplanets. Deep Lyα transits as observed with *Hubble Space Telescope* (*HST*)/STIS have suggested the presence of extended atmospheres on the hot Jupiters HD 209458b, which orbits a Sun-like star (Vidal-Madjar et al. 2003, 2004; Ben-Jaffel & Sona Hosseini 2010; Linsky et al. 2010) and HD 189733b which orbits a more active K1 dwarf (Lecavelier Des Etangs et al. 2010, 2012; Bourrier et al. 2013). Along with neutral hydrogen the presence of heavier elements have also been inferred in the upper atmosphere of HD 209458 in the FUV lines of O I (130.4 nm), C II (133.5 nm), Si III (120.6 nm), Si IV (139.8 nm), and Mg I (285.2 nm; Vidal-Madjar et al. 2004; Linsky et al. 2010;

Schlawin et al. 2010; Ben-Jaffel & Ballester 2013). Poppenhaeger et al. (2013) reported a tentative detection of HD 189733b in X-rays (0.1–6.3 nm) through multiple observations using *Chandra*. Due to the difficulty of observing X-ray transits and the activity of the star, Poppenhaeger et al. (2013) find an X-ray transit depth between 2.4% and 9%, i.e., 1–3 times the optical transit depth. Further observations will help determine if the X-ray transit depth of HD 189733b is indeed deeper than in the optical, or if it is the result of stellar activity.

Ehrenreich et al. (2012) reported a tentative detection of an extended atmosphere in Lyα of the warm Jupiter 55 Cancari b with a transit depth of $7.5 \pm 1.8\%$ detected with *HST*/STIS. This planet's transit has not been detected in optical photometry suggesting that if additional Lyα absorption is caused by the planet then the extended atmosphere is grazing the stellar disk. Lyα observations of GJ 436b's transit using *HST*/STIS have also revealed atmospheric escape from the atmosphere of this hot Neptune orbiting an M dwarf. Kulow et al. (2014) detected an absorption signature at the end of the optical transit of GJ 436b with a transit depth of ~25% (far greater than the 0.69% optical transit depth). A further study by Ehrenreich et al. (2015) determined the ephemeris time used by Kulow et al. (2014) to be inaccurate, and their reanalysis shifted this increased absorption signature into mid-transit. In their observations Ehrenreich et al. (2015) measured an even deeper asymmetric Lyα transit, with a depth of $56.3 \pm 3.5\%$ and found a cometary tail trailing the planet. Heavy UV radiation from the host stars is thought to have ionized the upper atmospheres of these planets, resulting in hydrodynamical blow-off (Murray-Clay et al. 2009; Tripathi et al. 2015), implying that these planets may have lost some of their atmosphere (Batalha et al. 2011; Pepe et al. 2013; Hu et al. 2015). Rugheimer et al. (2015) studied the effects of Lyα on Earth-like planets orbiting M dwarfs and found that even when the Lyα flux is increased to 180 times the largest

observed value in the MUSCLES stellar sample (France et al. 2013) it only has a small effect on the photochemistry of the planet's atmosphere. However, Miguel et al. (2015) showed that the impact of higher Lyα flux may drastically change the observable spectral features for mini-Neptunes in systems at lower pressures than those considered by Rugheimer et al. (2015).

NUV observations of the heavily irradiated hot Jupiter WASP-12b from *HST*/COS have revealed transit depths in the Mg II lines up to 3 times deeper than the optical transit depth (Fossati et al. 2010; Haswell et al. 2012). These transits also show an asymmetry in the timing of the transit, with their NUV (253.9–258.0 nm) events exhibiting an early ingress but ending simultaneously with the optical light curve. These deep transits have been attributed to the presence of heavy elements in the atmosphere of the planet; however, the early-ingress has also been attributed to the presence of a magnetospheric bowshock transiting ahead of the planet (Vidotto et al. 2010; Llama et al. 2011).

Observations of HD 189733b showed no detectable Lyα transit in 2010 April but detected a $14.4 \pm 3.6\%$ transit depth in 2011 September (Lecavelier Des Etangs et al. 2012). This transit depth is ~10 times deeper than the optical transit and has been attributed atmospheric blow-off from the planet. The changes in the transit depth are likely correlated to the variable stellar irradiation to which the planet is exposed.

Given that the variability and large depths observed in Lyα transits are being used to infer properties of exoplanet atmospheres, it is necessary to ask whether such variability could be directly attributed to stellar activity affecting the transit observation and not the presence of an extended atmosphere on the planet. Indeed, stellar activity effects must be accounted for when analyzing transit observations, particularly at short wavelengths since the presence of stellar active regions can alter the inferred transit depth and potentially lead to false conclusions about the composition of the planetary atmosphere. In the optical, dark star spots on the stellar surface that intersect the transit chord will result in a shallower transit as the planet occults less star light as it passes over the star spot. The presence of star spots that do not intersect the transit chord results in a deeper transit (e.g., Pont et al. 2013).

In Llama & Shkolnik (2015), we investigated the effect which both occulted and unocculted active regions have on exoplanetary transits in the soft X-ray, UV, and optical wavelengths by simulating transits over disk-resolved images of the Sun with the aim of determining whether stellar activity can mimic an extended planetary atmosphere. At short wavelengths, the active regions appear as extended, bright patches on the stellar disk, and therefore have the opposite effect than in the optical, i.e., the occultation of a bright region along the transit chord results in a deeper transit and the presence of unocculted X-ray/UV bright regions on the stellar disk will result in a shallower transit. Llama & Shkolnik (2015) showed that the impact of stellar activity was less prevalent at longer wavelengths (FUV and optical) due to the active regions being less extended than in the soft X-ray/EUV regime.

In this work, we used Lyα observations of the Sun taken continuously over 3.5 years to investigate the effect its variability has on our ability to recover the radius of a transiting exoplanet and aid the interpretations of Lyα transits of known exoplanets. We extracted 1100 continuous 3 hr windows of high cadence (10 s) Lyα data into which we
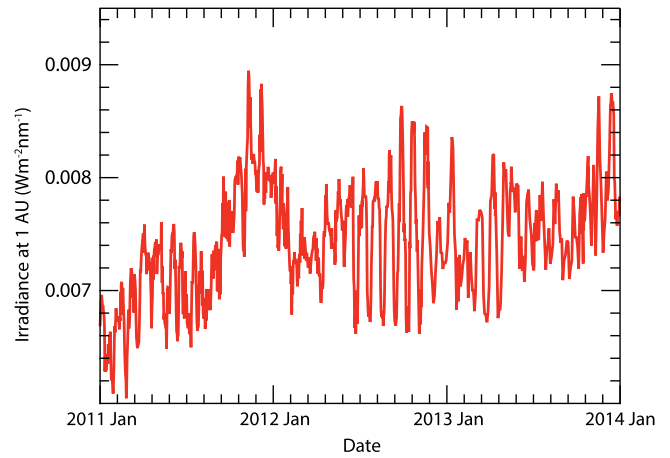

Figure 1. Lyα irradiance (adjusted to 1 AU) of the Sun (smoothed to 1 hr cadence) from 2011 January until 2014 January from the Extreme Ultraviolet Variability Experiment (EVE) instrument on board NASA's *Solar Dynamics Observatory* (*SDO*). The 27 day Solar rotation period can clearly be seen with variability of ~30%, as well as the transition from Solar minimum to Solar maximum.

inserted exoplanet transits. This enabled us to determine the effect of stellar activity on a single planet transit observation in Lyα, and to predict the number of transits needed to reliably measure the effective radius of the planet at this wavelength. To investigate the effects of stellar activity on more active stars, we scaled the Solar Lyα data to simulate light curves of higher variability stars such as HD 189733 and M dwarfs.

2. SOLAR OBSERVATIONS

2.1. Solar Dynamics Observatory (SDO)/EVE Observations

NASA's *SDO*[4] was launched in early 2010 and has been continuously monitoring the Sun at a range of wavelengths spanning the X-ray, UV, and optical. The Extreme Ultraviolet Variability Experiment (EVE)[5] instrument on board *SDO* measures the disk integrated (Sun-as-a-star) EUV spectrum once every 10 s within the wavelength range 6.5–37 nm using the Multiple EUV Grating Spectrograph (MEGS-A) component and also between 37 and 105 nm with the MEGS-B component (Woods et al. 2012). Additionally, the photo diode MEGS-P covers the Lyα emission feature. Although the bandpass of MEGS-P is 10 nm wide, 99% of the flux measured by this component is from the Solar Lyα emission (Woods et al. 2012). To minimize the instrument degradation, MEGS-P only acquires data at a 10 s cadence for 3 hr a day and for 5 minutes every hour the remainder of the time.

Using the IDL EVE routines from the Virtual Solar Observatory provided by SolarSoft[6], we downloaded all the available EVE level 2 line data. These files contain the Solar irradiance (adjusted to 1 AU) at selected emission lines, including Lyα. Figure 1 shows the Solar Lyα irradiance (as measured using MEGS-P) from 2011 January to 2014 January smoothed to a cadence of 1 hr. During this time the Sun was transitioning from Solar minimum toward maximum.

There are two forms of variability present in this light curve. First, long term rotational modulation caused by the 27 day
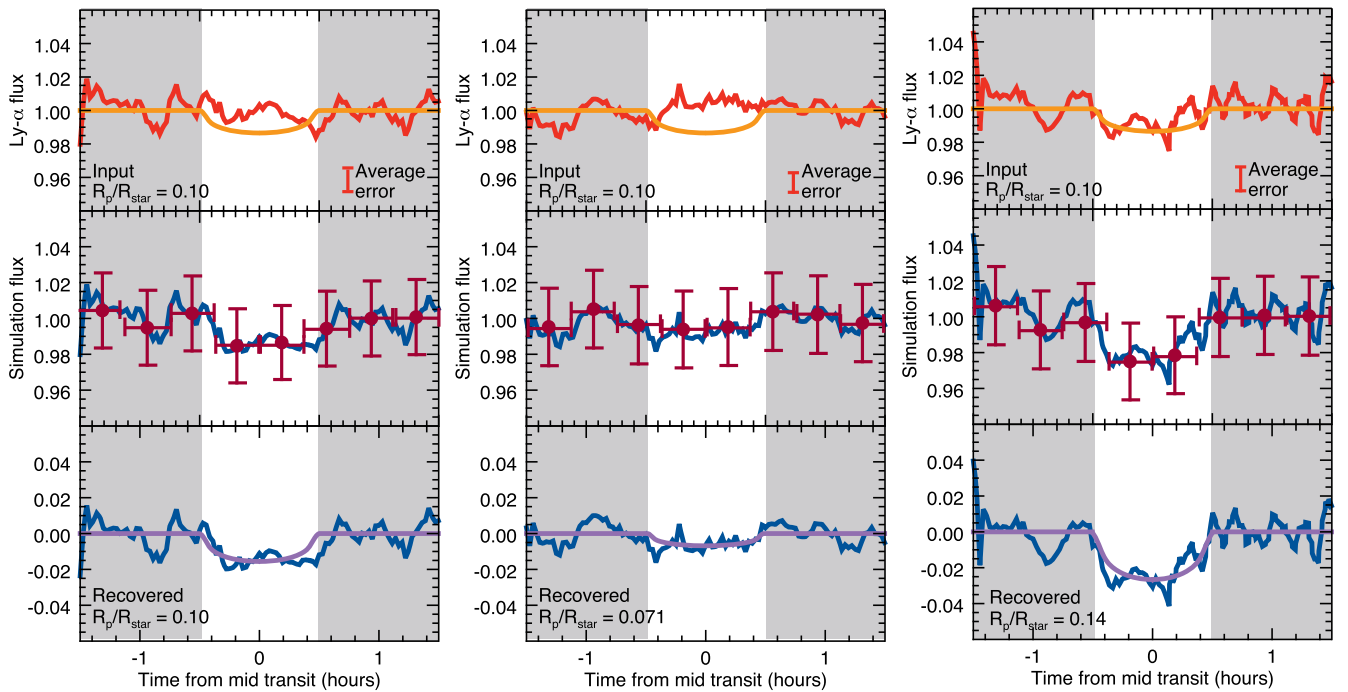
---

[4] http://sdo.gsfc.nasa.gov
[5] http://lasp.colorado.edu/home/eve/
[6] http://www.lmsal.com/solarsoft

Figure 2. Three of the 1100 simulations. The top panel shows the normalized 3 hr Lyα light curve (red) and the input model transit light with $R_{\rm p}/R_\star = 0.1$ curve (orange). The middle panel shows the combined Lyα and model transit light curve (blue). Over plotted is this light curve rebinned to a cadence similar to that of existing Lyα observations (see Section 5.3). We then fit a transit model to find the best-fit value of $R_{\rm p}/R_\star$ (purple). The first column shows an example where we recover the input value of $R_{\rm p}/R_\star$, the middle column shows an example where we recover a smaller value of $R_{\rm p}/R_\star$, and finally an example where $R_{\rm p}/R_\star$ is larger than the input value.

Solar rotation period can clearly be seen. This modulation, while varying by up to ∼30% is not problematic for transit observations, which are taken over the period of a few hours and so such long term variability will have an almost uniform effect on the light curve. Second, there is the presence of short term variability, caused by the evolution of the active regions themselves. This short term variability is more problematic when dealing with short observing windows since it affects the determination of the normalization level. It is the effect of this variability that degrades our ability to recover accurate values of the planet-to-star radius ratio, $R_{\rm p}/R_\star$.

Also on board *SDO* is the Atmospheric Imaging Assembly (AIA). This instrument monitors the Sun in ten wavelengths ranging from soft X-ray/EUV through to the near-ultraviolet and optical. Unlike EVE, this instrument records resolved images of the Solar disk with a spatial resolution of $1''$ on a CCD of 4096 px^2. These data were used in Llama & Shkolnik (2015) to simulate exoplanet transit light curves using disk resolved data. We found that the presence of large, bright, unocculted active regions on the Solar surface affect the normalization of the simulated transit chord and makes accurately measuring $R_{\rm p}/R_\star$ challenging in the soft X-ray/EUV regime. Here, we used disk integrated Lyα data and although we lose all spatial information, we provide the limits of probing the upper atmospheres of planets at key spectral signatures.

3. TRANSIT MODEL

The EVE MEGS-P Lyα data contains 3 hr of continuous observations per day (at 10 s cadence), setting the duration limit of our simulated transit events. We began by isolating the 3 hr of continuous data and rebinning it to 1 minute cadence for each day in our data set. In total we were able to isolate 1100 separate 3 hr windows of continuous Lyα data. Sample Lyα light curves are shown in the top panels of Figure 2 in red.

At the Lyα wavelength, the Sun is limb-darkened (e.g., Curdt et al. 2008), and so we simulated the transit light curve of a hot Jupiter with $R_{\rm p}/R_\star = 0.1$ at an impact parameter of $b = 0$ using the code developed by Mandel & Agol (2002). The 3 hr simulated transit light is comprised of the 1 hr transit event and 1 hr on either side of the transit.

The simulated transit light curve is plotted in the top panels of Figure 2 in orange. The Lyα light curve is then multiplied together with the model transit light curve to produce the simulated data so that only the in-transit part of the Lyα light curve is affected. The solid line in the middle panels of Figure 2 shows the results of multiplying the light curves together.

Using the simulated Lyα transit light curves we measured $R_{\rm p}/R_\star$ by performing a χ^2 test with simulated Mandel & Agol (2002) light curves with varying values of $R_{\rm p}/R_\star$ to find the best-fit transit light curve. For each case shown in Figure 2 the best-fit transit is shown in purple in the bottom panels. The impact parameter in our fitted light curves is fixed to the input value of $b = 0$ since this would be known from optical photometry. We also assumed the same limb-darkening coefficients as the input transit model, meaning the only free parameter in our fit is $R_{\rm p}/R_\star$.

4. RESULTS: LYα TRANSIT VARIABILITY

We repeated the process outlined in Section 3 and simulated 1100 transits of $R_{\rm p}/R_\star = 0.1$ using each of the isolated 3 hr windows of the Solar Lyα light curve. For each simulation we then recorded the measured value of $R_{\rm p}/R_\star$ to quantify the effects of Lyα variability on our ability to measure $R_{\rm p}/R_\star$. The
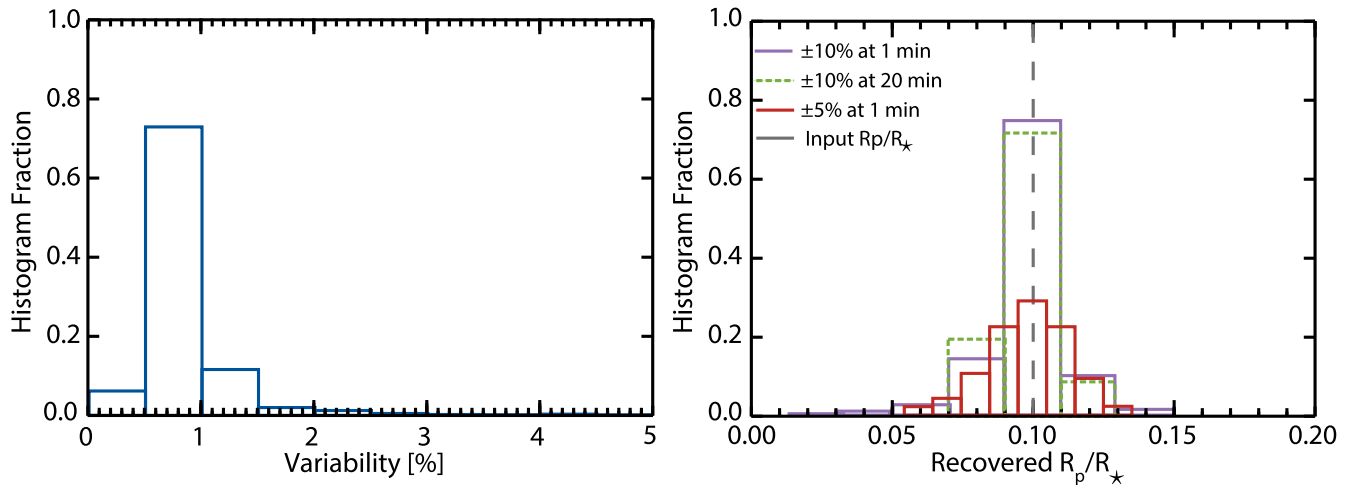
Figure 3. Left: histogram showing the short-term variability, defined as σ/μ (per light curve). Right: histogram of measured $R_p/R_\star$ from the 1100 simulated exoplanet transits of a hot Jupiter with $R_p/R_\star = 0.1$ into the Solar Lyα light curves. The $\pm 5\%$ bin width of the red histogram matches the binning presented in Llama & Shkolnik (2015), while the $\pm 10\%$ bin width of the purple histogram matches typical Lyα and X-ray transits. The dashed green line shows the distribution of $R_p/R_\star$ for the lower cadence observations (see Section 5.3).

simulation shown in Figure 2 (left column) is an example of where the input value of $R_p/R_\star = 0.1$ was recovered successfully. In this case, the Lyα variability during the 3 hr observing window was relatively small. The simulation in the middle column shows an example where the measured value of $R_p/R_\star$ is smaller than the input value, due to a large amount of short term variability in the light curve. The simulation in the right panel of Figure 2 is another example where there is significant short term variability in the Lyα light curve during the transit event, this time resulting in the best-fit model transit being one with a larger value of $R_p/R_\star$.

The left panel of Figure 3 shows a histogram of the variability present in the 3 hr windows of Lyα Solar data. We use the "coefficient of variance," σ/μ, where σ is the standard deviation and μ is the mean of the 3 hr data to compute the variability in the light curve. We find that during a 3 hr window, the Lyα variability does not exceed 3%, with 95% of the windows showing less than 1.5% variability.

The right panel of Figure 3 shows a histogram of the measured values of the planet-to-star radius ratio, $R_p/R_\star$, from the 1100 simulations. In all cases the input value was $R_p/R_\star = 0.1$. The red histogram has a bin width of $\pm 5\%$ to match the results presented in Llama & Shkolnik (2015), while the bin size of the purple histogram was chosen to match the typical $\pm 10\%$ uncertainties of Lyα and X-ray transits. Both histograms peak at the correct value of $R_p/R_\star = 0.1$ (within error). For the larger uncertainty histogram (purple), we find the correct answer is found with a frequency of $\sim$75%, while for the smaller uncertainty histogram (red), we find the input value with a frequency of $\sim$30%. The maximum value of $R_p/R_\star$ in our simulations is 50% larger than the input value which cannot explain the large transit depths for both HD 189733b and GJ 436b (Ehrenreich et al. 2012; Bourrier et al. 2013; Kulow et al. 2014).

5. DISCUSSION

5.1. 55 Cancari b: the Transit of a Planetary Exosphere

Ehrenreich et al. (2012) reported a tentative detection of 55 Cancari b, a planet previously only found in radial velocity. They reported a Lyα transit depth of $7.5 \pm 1.8\%$, suggesting

that if this absorption is from the planet, then this system may have a partially transiting exosphere. Using our Lyα light curves we were able to test this theory. We repeated the simulations as described in Section 3, this time without inserting an exoplanet transit. We then measured the best-fit $R_p/R_\star$ value to determine whether stellar activity alone can mimic a transit event. From the 1100 simulations, 65% of the light curves are best fit with no transit, and the median value of $R_p/R_\star = 0.02$, much smaller than the Lyα depth reported for 55 Cancari b by Ehrenreich et al. (2012). This finding strengthens the conclusion that the increased Lyα absorption that coincides with the transit of 55 Cancari b is unlikely caused by stellar activity but by the planet having an extended atmosphere that is partially transiting the stellar disk.

5.2. Comparison with Disk Resolved Data

In Llama & Shkolnik (2015) we were able to make use of disk resolved images of the Sun obtained by AIA and to account for both occulted and unocculted active regions in the simulated light curves, rather than the disk-integrated data as collected by EVE. We carried out two sets of simulations over the 10 wavelengths observed by AIA, 1 where the planet transited over the activity belts of the Sun ($b = -0.3$), and 1 where the planet transited over the equator ($b = 0$). In the first case, on average, we measured a larger value of $R_p/R_\star$ than the input value due to the planet frequently occulting active regions. In the latter case, the presence of unocculted active regions on the stellar surface meant that the transit depth was on average shallower, resulting in a smaller value of $R_p/R_\star$ being measured. The blue and red histograms shown in Figure 4 show the measured $R_p/R_\star$ distribution for the soft X-ray (9.4 nm) $b = 0$ and $b = -0.3$ simulations, respectively.

Multiple studies of the HD 189733 system have confirmed that the lack of bumps (caused by the planet occulting a star spot) in the transit light curve indicates it is unlikely that the transit chord is intersecting the activity belts of the star (Pont et al. 2013; Poppenhaeger et al. 2013).

Here, we do not have information on the locations of the star spots; however, the EVE data set also contains the same EUV data from AIA but as disk-integrated rather than disk-resolved
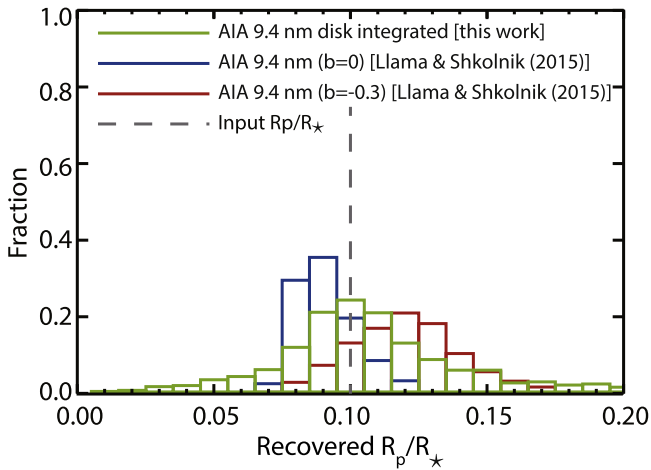
Figure 4. Histogram showing the distribution of measured $R_p/R_\star$ using the disk integrated AIA 9.4 nm data (green). Over plotted is the measured $R_p/R_\star$ from the transit simulations over the disk resolved AIA 9.4 nm data as shown in Figure 7 of Llama & Shkolnik (2015).

Figure 5. Histogram showing the distribution of measured $R_p/R_\star$ from combining 2, 5, and 10 separate transits together. Combining transits together improves the distribution of $R_p/R_\star$ with the correct answer being obtained in 90% of the simulations once more than 10 transits are combined.

data. This allows us, at least for the EUV wavelengths, to directly compare the simulation method used here with that presented in Llama & Shkolnik (2015). It is worthy of note that the 9.4 nm soft X-ray images of the Sun are limb-brightened rather than limb-darkened, meaning the transit light curve exhibits a W-shape rather than a U-shape. We therefore used a limb-brightened transit model (originally developed by Schlawin et al. 2010) rather the limb-darkened model shown here. For a full description of the limb-brightened model please see Section 3.3 of Llama & Shkolnik (2015).

The green histogram in Figure 4 shows the distribution of measured $R_p/R_\star$ using the disk integrated AIA 9.4 nm data and the simulation method presented in Section 3 (but using a limb-brightened transit model). The histogram shows that the spread in $R_p/R_\star$ is more symmetric about the correct value of $R_p/R_\star = 0.1$ for the disk integrated data and has a similar spread to the results where we used disk resolved data; however, since we were unable to simulate the effects of the planet directly occulting active regions this method provides a lower limit to the effects of activity on Lyα transit observations.

5.3. Lower Cadence of Observation

The histogram of measured $R_p/R_\star$ shown in Figure 3 was created using the Lyα light curve binned to a 1 minute cadence. Observations of exoplanet transits require longer integration times to obtain sufficient signal to noise and so are comprised of fewer data points. Llama & Shkolnik (2015) found that for the lower cadence light curves, the soft X-ray and EUV transit depths were on average shallower than in the high cadence case. To investigate the impact of longer integration times on the simulations presented here, we rebinned our 1100 Lyα transit light curves to a cadence of 20 minute so that each transit event (including out-of-transit) was comprised of 9 data points, rather than 180 at 1 minute cadence. Sample rebinned light curves are shown as data points in the middle panel of Figure 2. For each of these rebinned light curves we also measured the best-fit value of $R_p/R_\star$. We found a similar trend to that reported by Llama & Shkolnik (2015), where the measured value of $R_p/R_\star$ is lower than the full cadence simulations. The dashed histogram in Figure 3 shows the
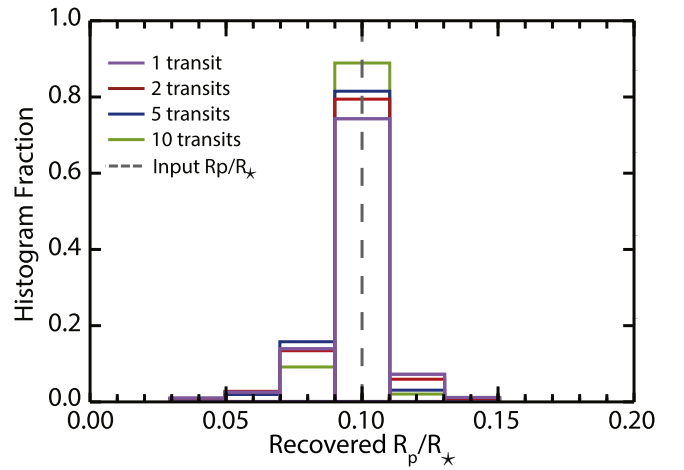
distribution of measured $R_p/R_\star$ for the lower cadence simulations.

5.4. Combining Data from Multiple Transits

Poppenhaeger et al. (2013) observed X-ray (0.1–6.3 nm) transits of HD 189733b using *Chandra*. By combining multiple transits they were able to determine an X-ray transit depth between 2.4% and 9%, i.e., 1–3 times deeper than the optical transit. Between these observations the distribution of star spots on the surface of the star will have changed, which will impact the transit recovery. To test how stellar activity will impact multiple transit observations we carried combined multiple Lyα light curves and measured the resultant $R_p/R_\star$ value. Figure 5 shows the results of combining multiple transits, which are chosen at random and then measuring the value of $R_p/R_\star$. For 2 transits, the correct value of $R_p/R_\star$ is measured in 80% of the simulations, and after 10 transits the correct value is obtained in 90% of the cases. We therefore conclude that despite stellar activity changes on the surface of the star, combining multiple transits increases the likelihood of measuring the correct value of $R_p/R_\star$, at least 90% of the time.

5.5. Simulating More Active Stars

Bourrier et al. (2013) reported a 14.4 ± 3.6% depth in the Lyα transit of HD 189733b in 2011 April, which is ~10 times deeper than the optical transit. Ben-Jaffel & Ballester (2013) reported an early ingress and increased absorption at multiple FUV wavelengths during transits of HD 189733b using *HST*/COS. They analyzed the O I, C II, Si IV, and Si III lines. In their O I light curve they found a transit depth consistent with $R_p/R_\star = 1.7\times$ the optical radius. Ben-Jaffel & Ballester (2013) carried out a short-term analysis of the activity on HD 189733 using the O I line in their data. They found that during their 5 hr observing campaign the FUV variability of HD 189733 was ~5%. Ehrenreich et al. (2015) carried out an analysis of the unabsorbed red-wing of the Lyα line in their GJ 436 observations and estimated the activity to vary by 5%–11% during a single visit.

From our histogram of short term Lyα variability (left panel of Figure 2) we find the Sun is less variable than HD 189733,
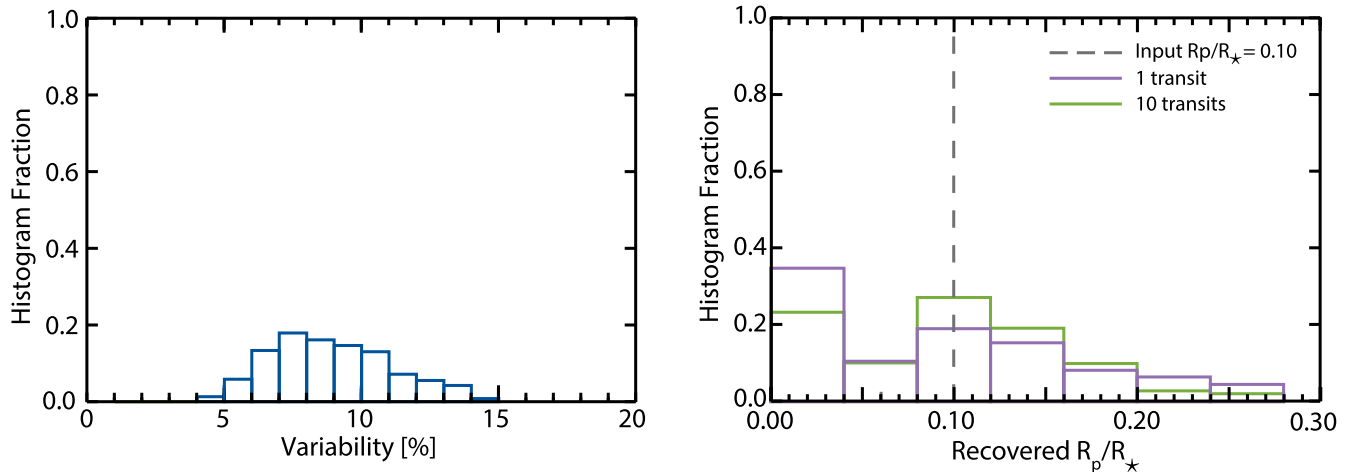
Figure 6. Left: histogram showing the variability, defined as σ/μ (per light curve), for the simulated higher activity Lyα data. Now the variability ranges from 5% to 15%, similar to the variability levels reported for HD 189733 and GJ 436 (Ben-Jaffel & Ballester 2013; Ehrenreich et al. 2015). Right: histogram of measured $R_{\rm p}/R_{\star}$ for the 1100 light curves using the simulated higher activity data (purple). For the higher amplitude data, we find ~35% of the simulated light curves are best fit with no transit. By combining 10 or more transits (green histogram) we find that the histogram then peaks at the correct answer of $R_{\rm p}/R_{\star} = 0.1$.

with 95% of our Lyα light curves showing less than 1.5% variability. To investigate the effect of a higher level of variability on our simulations we scaled the Solar Lyα light curve to attain variability levels comporabale to HD 18733 and GJ 436. To achieve this we took the normalized Lyα flux for each of the 1100 3 hr sets of observations and raised it to the tenth power. We note that this does not change the timescale of the variability, it only increases the overall amplitude of the variability. The left panel of Figure 6 shows the new variability distribution for the higher variability data, again defined as σ/μ. The variability now ranges between ~5% and 15%, similar to the short term variability estimates for HD 189733 and GJ 436.

The right panel of Figure 6 shows the distribution of measured $R_{\rm p}/R_{\star}$ for this data set obtained using the same method presented in Section 3. The purple histogram shows the distribution of $R_{\rm p}/R_{\star}$ for a single observation has a larger spread in measured values of $R_{\rm p}/R_{\star}$ than for the Solar variability data set. Almost 40% of the simulations are best fit by the no transit model, i.e., the variability is much larger than the transit depth.

In all 1100 of the higher variability simulations, we did not measure a value of $R_{\rm p}/R_{\star}$ large enough to produce the 56.3% transit depth reported for GJ 436b, again suggesting that the large Lyα transit depth of GJ 436 detected by Kulow et al. (2014) and Ehrenreich et al. (2015) is unlikely to be a mimic of stellar activity but rather supports the conclusion that this planet hosts an extended atmosphere. We also combined data sets to investigate the value of repeated transit observations. We find a large number of transits (>10) are required before the histogram peaks at the correct value of $R_{\rm p}/R_{\star} = 0.1$. We emphasize that the results presented in this Section are based on artificially boosting the variability in the Solar Lyα light curve and do not alter the timescale of the variability.

6. SUMMARY

Lyα transit observations provide the opportunity to probe the outermost atmospheres of exoplanets. However, at these wavelengths the impact of stellar activity is more prevalent than in the optical and infra-red and so must be accounted for when analyzing X-ray and UV observations to ensure an accurate measurement of the planet-to-star radius is obtained. At these high-energy wavelengths, active regions appear much brighter than their surroundings and evolve on a faster timescale than star spots in the optical.

Here we have used the Solar Lyα light curve obtained through the EVE instrument on board NASA's *SDO* spacecraft and inserted synthetic transits in an effort to determine how reliably we can measure the input planetary radius in the presence of stellar activity. We found that for stars of similar activity levels to that of our Sun, ~75% of Lyα transits will recover the true depth of the transit (to within ±10%). We investigated the effect of longer integration times and found that on average the measured value of $R_{\rm p}/R_{\star}$ will be smaller due to active regions being confined regions on the stellar disk; however, this effect is relatively small. For stars more active than the Sun, such as HD 189733 and most M dwarfs, our results serve as lower limits to the extent to which stellar activity will impact the ability to accurately recover the true planet-to-star radius ratio in Lyα observations.

We also ran simulations without inserting an exoplanet transit to test whether stellar activity alone can mimic an exoplanet transit. We found that 65% of the simulated light curves were best fit with no transit. In the remaining light curves we found no cases where the transit depth was comparable to the large depth found by Ehrenreich et al. (2012) that coincides with the transit of 55 Cancari b. This strengthens the conclusions that this planet does indeed have a partially transiting exosphere.

By artificially boosting the amplitude of the variability in the Solar Lyα light curve to the levels reported for HD 189733 and GJ 436 we found that 40% of the simulations are best fit with no transit and only after 10 observations does the distribution of $R_{\rm p}/R_{\star}$ peak at the correct value. However, we did not measure a value large enough to explain the large Lyα transit depths reported for GJ 436b by Kulow et al. (2014) and Ehrenreich et al. (2015), supporting the conclusion that this planet does indeed have an extended atmosphere. The findings and analyses presented here will be of particular importance when attempting to characterize the atmospheres of potentially habitable planets around M dwarfs.

REFERENCES

Batalha, N. M., Borucki, W. J., Bryson, S. T., et al. 2011, ApJ, 729, 27
Ben-Jaffel, L., & Ballester, G. E. 2013, A&A, 553, A52
Ben-Jaffel, L., & Sona Hosseini, S. 2010, ApJ, 709, 1284
Bourrier, V., Lecavelier Des Etangs, A., Dupuy, H., et al. 2013, A&A, 551, A63
Curdt, W., Tian, H., Teriaca, L., Schühle, U., & Lemaire, P. 2008, A&A, 492, L9
Ehrenreich, D., Bourrier, V., Bonfils, X., et al. 2012, A&A, 547, A18
Ehrenreich, D., Bourrier, V., Wheatley, P. J., et al. 2015, Natur, 522, 459
Ehrenreich, D., Lecavelier Des Etangs, A., & Delfosse, X. 2011, A&A, 529, 80
Fossati, L., Haswell, C. A., Froning, C. S., et al. 2010, ApJL, 714, L222
France, K., Froning, C. S., Linsky, J. L., et al. 2013, ApJ, 763, 149
Haswell, C. A., Fossati, L., Ayres, T., et al. 2012, ApJ, 760, 79
Hu, R., Seager, S., & Yung, Y. L. 2015, ApJ, 807, 8
Kulow, J. R., France, K., Linsky, J., & Parke Loyd, R. O. 2014, ApJ, 786, 132
Lecavelier Des Etangs, A., Bourrier, V., Wheatley, P. J., et al. 2012, A&A, 543, L4
Lecavelier Des Etangs, A., Ehrenreich, D., Vidal-Madjar, A., et al. 2010, A&A, 514, A72
Linsky, J. L. 1980, ARA&A, 18, 439
Linsky, J. L., Yang, H., France, K., et al. 2010, ApJ, 717, 1291
Llama, J., & Shkolnik, E. L. 2015, ApJ, 802, 41
Llama, J., Wood, K., Jardine, M., et al. 2011, MNRAS Letters, 416, L41
Mandel, K., & Agol, E. 2002, ApJL, 580, L171
Miguel, Y., Kaltenegger, L., Linsky, J. L., & Rugheimer, S. 2015, MNRAS, 446, 345
Murray-Clay, R. A., Chiang, E. I., & Murray, N. 2009, ApJ, 693, 23
Pepe, F., Cameron, A. C., Latham, D. W., et al. 2013, Natur, 503, 377
Pont, F., Sing, D. K., Gibson, N. P., et al. 2013, MNRAS, 432, 2917
Poppenhaeger, K., Schmitt, J. H. M. M., & Wolk, S. J. 2013, ApJ, 773, 62
Rugheimer, S., Kaltenegger, L., Segura, A., Linsky, J., & Mohanty, S. 2015, ApJ, 809, 57
Schlawin, E., Agol, E., Walkowicz, L. M., Covey, K., & Lloyd, J. P. 2010, ApJL, 722, L75
Shkolnik, E. L., & Barman, T. S. 2014, AJ, 148, 64
Tripathi, A., Kratter, K. M., Murray-Clay, R. A., & Krumholz, M. R. 2015, ApJ, 808, 173
Vidal-Madjar, A., des Etangs, A. L., Désert, J.-M., et al. 2003, Natur, 422, 143
Vidal-Madjar, A., Dsert, J. M., Etangs, A. L. d., et al. 2004, ApJL, 604, L69
Vidotto, A. A., Jardine, M., & Helling, C. 2010, ApJL, 722, L168
Woods, T. N., Eparvier, F. G., Hock, R., et al. 2012, SoPh, 275, 115